Equal channel angular pressing processing routes and associated structure modification: a differential scanning calorimetry and X-ray line profile analysis

A. Sarkar,[1,a)] Satyam Suwas,[1] D. Goran,[2] J.-J. Fundenberger,[2] L.S. Toth,[2] and T. Grosdidier[2]
[1]Department of Materials Engineering, Indian Institute of Science, Bangalore 560012, India
[2]LEM3, Université Paul Verlaine de Metz, Ile du Saulcy, 57045 Metz Cedex 1, France

The effectiveness of different routes of equal channel angular pressing (A, B_c, and C) is studied for commercially pure copper. The stored energy and the activation energy of recrystallization for the deformed samples were quantified using differential scanning calorimetry and X-ray diffraction line profile analysis. Results of the study revealed that the dislocation density and the stored energy are higher in the case of route B_c deformed sample. The activation energy for recrystallization is lower for route B_c. © 2012 International Centre for Diffraction Data [doi:10.1017/S0885715612000310]

I. INTRODUCTION

Severe plastic deformation (SPD) is now a well-established methodology for the processing of bulk ultrafine grained materials. The principle of SPD includes increasing dislocation density by heavily deforming materials, formation of dense dislocation walls, and transforming dislocation walls into high-angle grain boundaries (Valiev *et al.*, 2000). Among various SPD techniques, equal channel angular pressing (ECAP) is the most popular technique to generate ultrafine grain sizes bulk materials (Segal, 1995; Valiev, 1997; Alexandrov *et al.*, 1998; Stolyarov *et al.*, 1999). During the ECAP process, a simple shear deformation is imposed on the material when passed through two intersecting channels of equal cross-sectional area (Segal, 1995). Since the size of work piece remains unchanged after the pressing, this process can be, in principle, repeated for an indefinite number of times to tailor microstructure and strength (Segal, 1995; Valiev, 1997; Alexandrov *et al.*, 1998; Stolyarov *et al.*, 1999).

In the multiple pass deformation technique there is a possibility to introduce a variety of strain path change, each of which is designated as a specific route of ECAP. Therefore, the processing route is an important parameter that would strongly influence the microstructural evolution. Generally, three routes in the ECAP pressing are usual: route A, without any rotation of the sample around its axis upon repeated deformation; route B_c, with sequential rotation of the sample by 90° around its axis; and route C, with the rotation of sample by 180° around its axis during repeated deformation (Valiev *et al.*, 2000). We have previously reported the influence of processing route on texture evolution in commercially pure aluminum (Suwas *et al.*, 2005, 2009) and also the influence of processing routes on recrystallization in copper (Suwas *et al.*, 2004; Suwas and Kim, 2007). However, these studies were qualitative and did not reveal all aspects of microstructural evolution. The aim of the present study is to investigate the effect of processing route on the microstructural evolution in more quantitative manner and comment on the efficiency of the processing route, with regard to further stability of the microstructure, which is a major concern now. The study has been focused on commercially pure copper, as the previous investigations (Suwas *et al.*, 2006; Skrotzki *et al.*, 2007) have shown the formation of stable deformation microstructures and the characteristic deformation patterns indicated though ideal texture formation for this material.

II. EXPERIMENTAL

A. Processing

An extruded bar of commercial purity copper was subjected to annealing at 350 °C for 1 h to obtain strain-free microstructure with equiaxed grain. Specimens with dimensions of 100 mm × 10 mm × 10 mm were machined from the annealed bar. The ECAP experiments were carried out at a cross head speed of 1 mm s^{-1} at room temperature using a Zwick 200 kN screw driven machine. A specially designed die (Mathieu *et al.*, 2006) with square cross section of the extrusion channels (90°) was used. The specimens were subjected to ECAP up to four passes following routes A, B_c, and C.

B. Differential scanning calorimetry (DSC)

To estimate the amount of stored energy of cold work and the recrystallization temperature, DSC was carried out for each of the deformed samples. As it is well established that strain heterogeneities develop in ECAP processed samples because of different amount of friction along the die walls (Suwas *et al.*, 2006; Skrotzki *et al.*, 2007), only the central part of the billets has been investigated. Therefore, the DSC analysis was carried out on cubical samples (2 mm × 2 mm × 2 mm) cut from the central portion of each of the ECAP processed rods. These samples were then chemically polished using a solution of 30 ml of nitric acid, 10 ml of hydrochloric acid, 10 ml of phosphoric acid, and 50 ml of glacial acetic acid to remove any surface deformation that could have been

generated by the cutting procedure. The cubes were further cleaned in ethanol and dried before they were used for DSC. They were then placed in one of the two furnaces of a SETARAM DSC 131 Differential Scanning Calorimeter and analyzed at a constant heating rate of 20 K min^{-1}. A reference sample of well-annealed silver was placed in the other furnace. The power difference between the two furnaces, required to maintain the heating rate constant was recorded as a function of temperature. Recrystallization phenomenon is exothermic in nature and consequently results in peak in the DSC heat flow curve. The specimens were then cooled and reheated under identical conditions to establish a base line. The stored energy per unit mass is then the ratio of the area under the peak with respect to the sample weight.

Activation energy of recrystallization was calculated from the DSC measurements at different heating rates 5, 10, 15, and 20 K min^{-1}. The dependence of the peak temperature on the heating rate was used to calculate the apparent activation energy for recrystallization based on the Kissinger method (Kissinger, 1957). Kissinger analysis is used to determine the apparent activation energy (Q) for recrystallization.

$$\ln\left(\frac{V}{T_p^2}\right) = A - \frac{Q}{RT_p} \tag{1}$$

where V is the heat rate, T_p is the peak temperature, A is a constant, Q is the apparent activation energy, and R is the gas constant.

C. X-ray diffraction

Samples with an area of 8 mm × 8 mm were cut from the central portion of the deformed specimens and electro-polished for the X-ray diffraction experiments. The X-ray diffraction patterns were recorded from the polished surface by a PANalytical X'PertPro diffractometer using Cu K radiation. All the diffraction profiles were obtained by varying 2θ from 40° to 120° in a continuous scan mode. The data were recorded in a 2θ interval of 0.017°. The diffraction profiles were corrected for the instrumental broadening using a standard silicon sample, which had large crystallites and was free from the defects.

III. RESULTS

A. DSC measurement

Figure 1 shows the DSC thermograms of the deformed samples processed using routes A, B_c, and C. Peaks in the plot indicate the exothermic heat flow because of recrystallization. It is clear that the onset of recrystallization starts earlier for the route B sample. It can also be seen that for routes A and C the peaks are sharper compared with the samples deformed using route B_c. The area of the peak corresponds to the stored energy in the material and the values of the stored energy along with the recrystallization peak temperatures are reported in Table I for the different samples. The activation energy for recrystallization has been determined using the Kissinger analysis. Figure 2 shows the plot of $\ln(V/T_p^2)$ vs. $1/T_p$ for Kissinger analysis of the samples deformed for four passes using different routes. The slope of the curve corresponds to the activation energy of recrystallization (Q). The
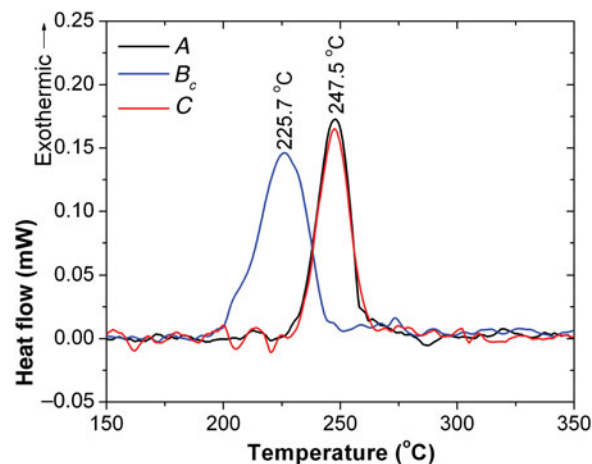

Figure 1. (Color online) DSC thermograms for Cu samples deformed up to four ECAP passes using different routes.

values of Q for different processing routes are reported in Table I. It can be seen that the Q value is minimum for the sample deformed using route B_c. The values of the stored energy and Q are of the same order of magnitude of conventionally deformed samples (Cao *et al.*, 2008).

B. XRD measurement

Figure 3 shows that the XRD traces obtained on the deformed samples using the three different routes. It is interesting to note that the relative intensities of the diffraction peaks are different for the three different processing routes. This indicates that a crystallographic texture has been produced during the ECAP deformation and that the nature of this texture is different depending on the exact processing route. A typical whole powder pattern fitting of the XRD profile of the sample deformed using route C is shown in Figure 4. Integral breadths of the peaks obtained from the fitting were used to draw the classical Williamson–Hall (WH) plot (Williamson and Hall, 1952). Figure 5 shows the classical WH plots for the three different samples. In the plots, ΔK ($=2\beta \cos\theta/\lambda$, β being the integral breadth) is plotted against K ($=2\sin\theta/\lambda$). It can be seen that the broadening is highly anisotropic, i.e. not a monotonic function of K for all the cases. The anisotropic broadening indicates the presence of a large amount of dislocations in the samples (Ungar and Borbely, 1996; Gubicza *et al.*, 2004, 2005; Ungar, 2004).

The dislocation-type factor q, dislocation density ρ, arrangement of dislocation M, as well as the median and variance of the size of coherently diffracting domains distribution of the ECAPed Cu were determined using the multiple whole powder (MWP) pattern fitting computer program (Ribárik *et al.*, 2001). The details of theoretical background of this

TABLE I. Results obtained from DSC study of four pass deformed samples.

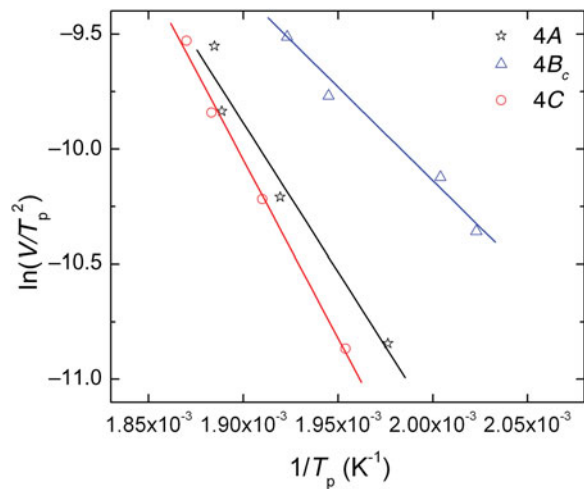| Route	Peak temperature (°C)	Stored energy (J g^{-1})	Activation energy (Q) kJ mol^{-1}
A	247.5	0.494	107
B_c	225.7	0.771	68
C	247.5	0.490	125

Figure 2. (Color online) Plot for Kissinger analysis to determine activation energy for Cu sample after four ECAP passes using different routes.

Figure 4. (Color online) Whole pattern fit of the XRD profile for Cu sample after four ECAP passes using route C.

method can be found in different literatures (Ungar and Tichy, 1999; Ungar et al., 1999; Ribárik et al., 2001). In this procedure, normalized Fourier transform of all the profiles after de-convolution were fitted simultaneously with those calculated according to the theoretical size and strain profile functions for a restrictedly random dislocation distribution (Wilkens, 1970a) and a log-normal distribution of spherical crystallites (Ribárik et al., 2001). In this program, the unit-cell parameter (a), Burgers vector (b) for the most common dislocation slip system and the average contrast factor of dislocation ($\bar{C}_{h00}$) as calculated from the ANIZC program (Borbely et al., 2003) are the non-refinable input parameters. The results of the MWP fitting procedure are shown in Table II. A typical fit of the intensity profile for 4C pass sample is shown in Figure 6. A good fit could be observed in the present case. From the table it is clear that the size of coherently diffracting domains is slightly smaller in the case of the sample deformed through route A compared with routes B_c and C. Table II further lists the parameters determining the type of dislocation (q) and dislocation arrangement parameter (M). The dislocation density of the different deformed samples is $\sim 10^{15}$ m^2. This corroborates the results obtained
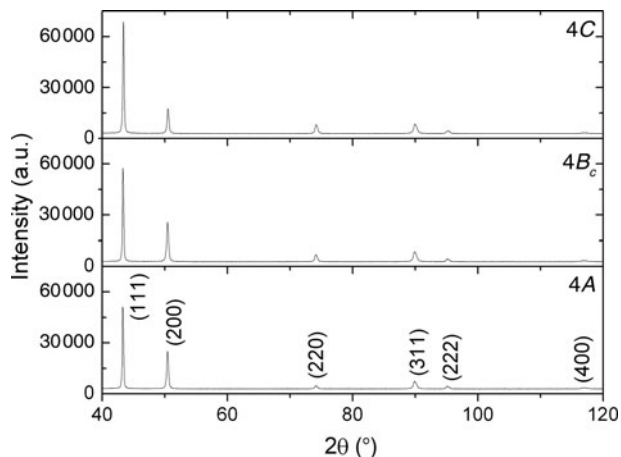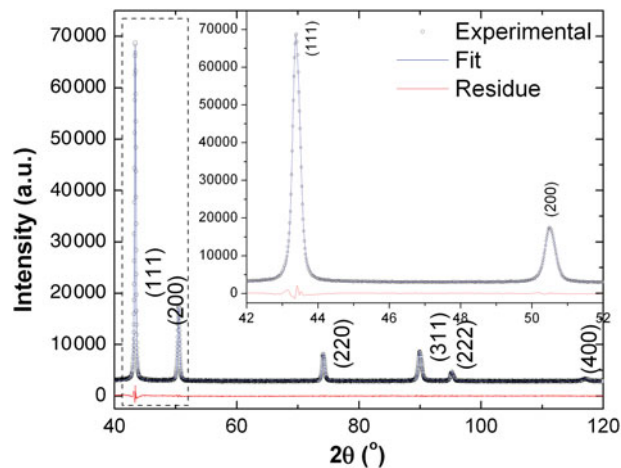
by other researchers (Gubicza et al., 2005; Schafler et al., 2005). In our case, the value of dislocation density is maximum in the case of sample deformed through route B_c. The stored energy (E) of the deformed materials can also be calculated from the ρ values using the relation:

$$E = 0.5\rho Gb^2 \qquad (2)$$

where G is the shear modulus. The calculated values of the stored energy are listed in Table II. Consistently with the results obtained by DSC, the XRD results indicate that the stored energy is maximum for the sample processed using the route B_c.

Values of the dislocation-type factor parameter q obtained from the MWP fit analysis are shown in Table II. Theoretical values of q for pure edge and pure screw-type dislocations for copper are 1.60 and 2.34, respectively, and for nearly equally populated screw and edge dislocation, the value comes out to be approximately 1.97 (Gubicza et al., 2001). The values experimentally obtained here for q indicate that the processing route changes the character of the dislocation. The dislocation structure is a combination of equally populated edge and screw type for route A, while the amount of edge-type dislocations increases for route B_c. Ultimately, the sample
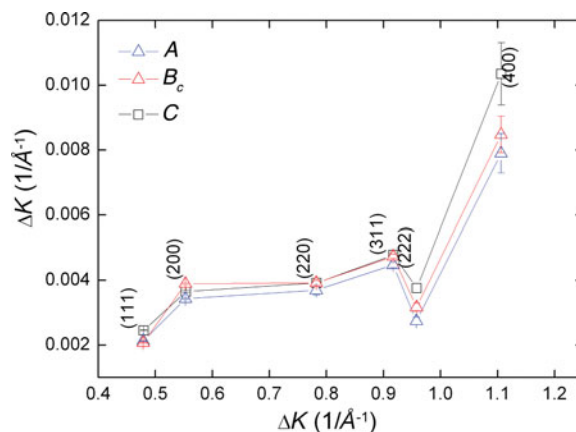

Figure 3. X-ray diffraction profiles for Cu sample after four ECAP passes using different routes.

Figure 5. (Color online) Classical Williamson–Hall plot for Cu samples after four ECAP passes using different routes.

Route	Crystallite size (nm)	Dislocation density (m^{-2})	Stored energy (E) (J g^{-1})	q	M
A	45	1.73×10^{15}	0.307	2.02	0.205
B_c	52	2.05×10^{15}	0.363	1.78	0.242
C	51	1.72×10^{15}	0.305	1.45	0.175

processed using route C is essentially characterized by dislocations of edge character. The dislocation arrangement parameter (M) is less than 1 for all the routes and is independent of the processing route. The values of arrangement parameters indicate that dislocations are highly correlated (Wilkens, 1970b). The crystallite size distribution functions for all different samples are shown in Figure 7. It is observed from the values of variance and median of size distribution that the distribution functions are narrower and sharper for routes A and B_c deformed samples compared with the sample deformed using route C.

VI. DISCUSSION

Nanostructured bulk materials can be produced by a number of processing methods. It has been found experimentally that the nanostructured metals produced by these techniques show a very high strength – typically several times higher than observed in coarse-grained materials – but a limited ductility of only a few percent of uniform elongation. For practical applications of nanostructured metals, it is therefore required to optimize the balance between strength and ductility. In a recent paper Wang and Ma (2004), have explored different ideas to remove or delay the plastic instabilities that hamper the useful ductility because of the presence of the nanostructure. The suggested stabilizing mechanisms were invoked by selecting appropriate tensile deformation conditions (such as deformation temperature and strain rate) or by tailoring the grain size structure to obtain bimodal or multi-modal grain size distributions (Wang et al., 2002; Wang and Ma, 2004). For the latter case, even if the number fraction of larger grains

in the nanostructure is low, their volume fraction can be sufficiently high to contribute to dislocation-based plasticity in the material (Ma, 2003). In addition, the thermal stability is also an important issue for the potential applications of nanostructured materials. Thus, when discussing the efficiency of the ECAP routes, it is important to consider that the effectiveness of a given route is directly related to the necessity of producing the most favorable microstructure associated with the required properties in the end products.

Despite the fact that all the ECAP routes lead to submicron-grained microstructures because of the high imparted strain, one of the interest of this technique is that the different routes of processing should help tailor the fine scale features of the microstructure – such as dislocation density, nature of grain boundary, and size distribution to achieve optimum mechanical properties. Some attempts have already been made in the literature to characterize the efficiency of the processing routes (Ferrasse et al., 1997; Oh-Ishi et al., 1998; Stolyarov et al., 2001; Li et al., 2006). Based on the experimental observation and the deformation modes involved, Stüwe (2003) speculated route A to be the most efficient in terms of storage of dislocations. However, earlier experimental studies showed the trend that the density of dislocation is higher in route B_c deformed sample (Langdon et al., 2000; Dobatkin et al., 2004). Dobatkin et al. (2007) examined the effect of the route and strain of ECAP on the structure and properties of oxygen-free copper pressed between $N = 5$ and 25 passes. They investigated the microstructure of the deformed samples by transmission electron microscopy (TEM) and orientation imaging microscopy (OIM) and also determined the mechanical properties. Their
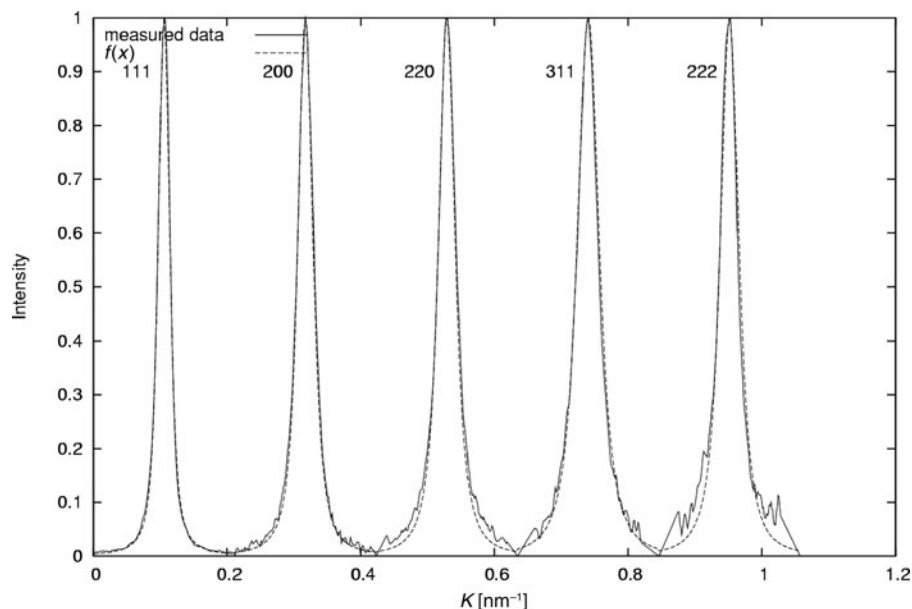

Figure 6. MWP fit of XRD intensity profile for Cu sample after four ECAP passes using route C.
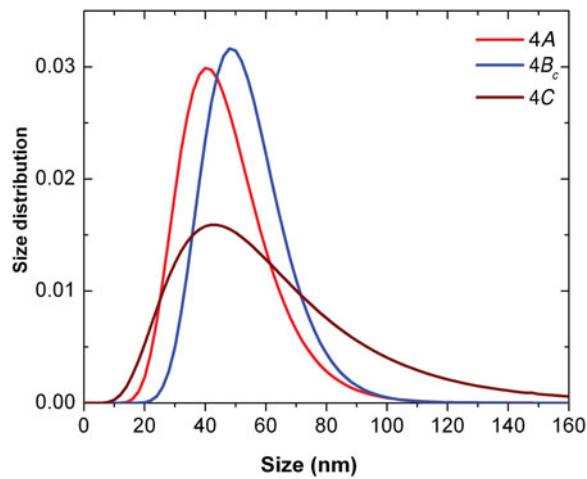
Figure 7. (Color online) Crystallite size distribution function for Cu samples after four ECAP passes using different routes.

study indicated that the size of the structural element virtually does not depend on the processing route. The yield strength (YS) was found to be higher in the case of the sample deformed using route B_c. One of the interesting result they found was that the strength properties remained essentially constant in the range of $N = 5–25$ passes, while – particularly for route B_c – the ductility could increase between $N = 10$ and $N = 25$. The authors suggested that this may be because of the presence of a bimodal-like structure (Dobatkin *et al.*, 2007). Grosdidier *et al.* also detailed the evolution of microstructure and corresponding tensile properties in high-purity copper processed using route B_c (Grosdidier *et al.*, 2010). Their analysis revealed that after sufficient strain deformation imparted to their commercial purity Cu samples (>12 passes using route B_c), a balance between recovery/recrystallization and deformation processes occurred during ECAP that generated a multi-modal grain size distribution in the sample. Again, this multi-modal grain size distribution generated the best strength – ductility compromise (Grosdidier and Llorca, 2010).

Results reported in the previous section as obtained from the DSC and XRD studies indicate that the stored energy is higher in the route B_c deformed sample compared with the routes A and C. The stored energy in the material is related to the amount of dislocations accumulated during processing which is directly related to the strength level of the processed materials. Thus, according to our results in terms of storage of dislocation, the strength of the sample deformed using route B_c should be higher. Dobatkin *et al.* (2007) have studied the properties of Cu samples processed using the three routes (A, B_c, and C) for increasing the amount of strain up to $\varepsilon = 29$. They found, indeed, that the samples processed following route B_c always revealed higher strength. Therefore, in terms of efficiency of the SPD process for imparting maximum dislocation in the material, route B_c is the most efficient route.

However, because of the high-stored energy, the microstructures obtained through SPD are far from equilibrium. This can be a detrimental feature regarding thermal stability of a material. Therefore, the thermal stability of the ECAP microstructure is important in terms of the practical application of the ECAP processed material. The activation energy of recrystallization of the deformed sample gives an indication

of the thermal stability. The result of the Kissinger analysis indicated that the activation energy is low for the route B_c deformed sample. Low activation energy corresponds to poor thermal stability of the deformed microstructure and, thus, samples processed through route B_c are the least thermally stable. Comparatively, routes A and C deformed sample microstructures have better thermal stability.

As discussed earlier the other important microstructural parameter that plays crucial role in determining mechanical properties of ultrafine grain materials is the distribution of crystallite size. It is now established from different studies that the broad crystallite size distribution yields better ductility. It has been observed that the crystallite size distribution is broader in the case of route C deformed sample compared with routes A and B_c. Hence route C sample is expected to show better mechanical property.

Thus, if we consider the efficiency of the route of ECAP taking into consideration the thermal stability and mechanical properties of deformed microstructure, route C seems to be better compared with the other two routes.

V. CONCLUSION

Based on DSC and XRD studies of the samples deformed through routes A, B_c, and C using ECAP, the following conclusions can be drawn:

1. Route B_c leads to maximum storage of dislocations in the sample deformed using ECAP. This leads to higher value of stored energy in this sample.
2. The activation energy for recrystallization is low for the route B_c deformed sample indicating the poor thermal stability of the deformed microstructure.
3. The crystallite size is smaller in the case of route A deformed sample and the size distribution is narrow in the case of routes A and B_c.
4. The character of dislocations present in the deformed sample is dependent on the processing route. Route A leads to a dislocation structure that is combination of equally populated edge and screw type, while for route B the edge-type dislocations are more. For route C samples, the dislocations are entirely of edge character.
5. The arrangement of dislocations is independent of the processing route. The dislocations are arranged in a highly correlated fashion in all the ECAPed samples.

Alexandrov, I. V., Islamgaliev, R. K., Valiev, R. Z., Zhu, Y. T., and LoweI, T. C. (**1998**). "Microstructures and properties of nanocomposites obtained through SPTS consolidation of powders," Metall. Mater. Trans. **A29**, 2253–2260.

Borbely, A., Dragomir, I., Ribarik, G., and Ungar, T. (**2003**). "Computer program *ANIZC* for the calculation of diffraction contrast factors of dislocations in elastically anisotropic cubic, hexagonal and trigonal crystals," J. Appl. Cryst. **36**, 160–162.

Cao, W. Q., Gu, C. F., Pereloma, E. V., and Davies, C. H. J. (**2008**). "Stored energy, vacancies and thermal stability of ultrafine grained copper," Mater. Sci. Eng. **A492**, 74–79.

Dobatkin, S. V., Kopylov, V. I., Pippan, R., and Vasil'eva, O. V. (**2004**). "Formation of high-angle grain boundaries in iron upon cold deformation by equal-channel angular pressing," Mater. Sci. Forum **467–470**, 1277–1282.

Dobatkin, S. V., Szpunar, J. A., Zhilyaev, A. P., Cho, J.-Y., and Kuznetsov, A. A. (**2007**). "Effect of the route and strain of equal-channel angular pressing on structure and properties of oxygen-free copper," Mater. Sci. Eng. **A462**, 132–138.

Ferrasse, S., Hartwig, K. T., Goforth, R. E., and Segal, V. M. (**1997**). "Microstructure and properties of copper and aluminum alloy 3003 heavily worked by equal channel angular extrusion," Metall. Mater. Trans. **A28**, 1047–1057.

Grosdidier, T., Goran, D., Ji, G. and Llorca, N. (**2010**). "On the processing of hetero-nanostructured metals for improved strength/ductility balance by ECAE and SPS techniques," J. Alloys Compd **504**, S456–S459.

Grosdidier, T. and Llorca, N. (**2010**). "Processing dense hetero-nanostructured metallic materials for Improved strength/ductility balance through high strain deformation and electrical current assisted sintering (ECAS)," Mater. Sci. Forum **633–634**, 559–567.

Gubicza, J., Balogh, L., Hellmig, R. J., Estrin, Y., and Ungar, T. (**2005**). "Dislocation structure and crystallite size in severely deformed copper by X-ray peak profile analysis," Mater. Sci. Eng. **A400–401**, 334–338.

Gubicza, J., Kassem, M., Ribárik, G., and Ungár, T. (**2004**). "The microstructure of mechanically alloyed Al–Mg determined by X-ray diffraction peak profile analysis," Mater. Sci. Eng. **A372**, 115–122.

Gubicza, J., Ribárik, G., Goren-Muginstein, G. R., Rosen, A. R., and Ungar, T. (**2001**). "The density and the character of dislocations in cubic and hexagonal polycrystals determined by X-ray diffraction," Mater. Sci. Eng. **A309–310**, 60–63.

Kissinger, H. E. (**1957**). "Reaction kinetics in differential thermal analysis," Anal. Chem. **29**, 1702–1706.

Langdon, T. G., Furukawa, M., Nemoto, M., and Horita, Z. (**2000**). "Using equal-channel angular pressing for refining grain size," JOM **52**(4), 30–33.

Li, S., Gazder, A. A., Beyerlein, I. J., Pereloma, E. V., and Davies, C. H. J. (**2006**). "Effect of processing route on microstructure and texture development in equal channel angular extrusion of interstitial-free steel," Acta Mater. **54**, 1087–1100.

Ma, E. (**2003**). "Instabilities and ductility of nanocrystalline and ultrafine-grained metals," Scr. Mater. **49**, 663–668.

Mathieu, J. P., Suwas, S., Eberhardt, A., Tóth, L. S., and Moll, P. (**2006**). "A new design for equal channel angular extrusion," J. Mater. Process. Technol. **173**, 29–33.

Oh-Ishi, K., Horita, Z., Furukawa, M., Nemoto, M., and Langdon, T. G. (**1998**). "Optimizing the rotation conditions for grain refinement in equal-channel angular pressing," Metall. Mater. Trans. **A29**, 2011–2013.

Ribárik, G., Ungár, T., and Gubicza, J. (**2001**). "*MWP-fit*: a program for multiple whole-profile fitting of diffraction peak profiles by *ab initio* theoretical functions," J. Appl. Cryst. **34**, 669–676.

Schafler, E., Steiner, G., Korznikova, E., Kerber, M., and Zehetbauer, M. J. (**2005**). "Lattice defect investigation of ECAP-Cu by means of X-ray line profile analysis, calorimetry and electrical resistometry," Mater. Sci. Eng. **A410–411**, 169–173.

Segal, V. M. (**1995**). "Materials processing by simple shear," Mater. Sci. Eng. A **197**, 157–164.

Skrotzki, W., Scheerbaum, N., Oertel, C.-G., Arruffat-Massion, R., Suwas, S., and Tóth, L. S. (**2007**). "Microstructure and texture gradient in copper deformed by equal channel angular pressing," Acta Mater. **55**, 2013–2024.

Stolyarov, V. V., Zhu, Y. T., Alexandrov, I. V., Lowe, T. C., and Valiev, R. Z. (**2001**). "Influence of ECAP routes on the microstructure and properties of pure Ti," Mater. Sci. Eng. **A299**, 59–67.

Stolyarov, V. V., Zhu, Y. T., Lowe, T. C., and Valiev, R. Z. (**1999**). "A two step SPD processing of ultrafine-grained titanium," NanoStruct. Mater. **11**, 947–954.

Stüwe, H. P. (**2003**). "Equivalent strains in severe plastic deformation," Adv. Eng. Mater. **5**, 291–295.

Suwas, S. and Kim, D.-I. (**2007**). "Annealing texture of ECAE processed copper," Mater. Sci. Forum, **558–559**, 1353–1358.

Suwas, S., Arruffat Massion, R., Tóth, L. S., Fundenberger, J.-J., and Beausir, B. (**2009**). "Evolution of texture during equal channel angular extrusion of commercially pure aluminum: Experiments and simulations," Mater. Sci. Eng. **A520**, 134–146.

Suwas, S., Arruffat Massion, R., Tóth, L. S., Fundenburger, J. J., Eberhardt, A., and Skrotzki, W. (**2006**). "Evolution of crystallographic texture during equal channel angular extrusion of copper: the role of material variables," Metall. Mater. Trans. **37A**, 739–753.

Suwas, S., Eberhardt, A., Tóth, L. S., Fundenberger, J. J., and Grosdidier, T. (**2004**). "A recrystallisation based investigation for efficiency of processing routes during equal channel angular extrusion," Mater. Sci. Forum, **467–470**, 1325–1332.

Suwas, S., Tóth, L. S., Fundenberger, J.-J., and Eberhardt, A. (**2005**). "Texture evolution in commercially pure Al during equal channel angular extrusion (ECAE) as a function of processing routes," Solid State Phenom., **105**, 357–362.

Ungar, T. (**2004**). "Microstructural parameters from X-ray diffraction peak broadening," Scr. Mater. **51**, 777–781.

Ungar, T. and Borbely, A. (**1996**). "The effect of dislocation contrast on X-ray line broadening: a new approach to line profile analysis," Appl. Phys. Lett. **69**, 3173–3175.

Ungar, T. and Tichy, G. (**1999**). "The effect of dislocation contrast on X-ray line profiles in untextured polycrystals," Phys. Status Solidi a **171**, 425–434.

Ungar, T., Dragomir, I., Revesz, A., and Borbely, A. (**1999**). "The contrast factors of dislocations in cubic crystals: the dislocation model of strain anisotropy in practice," J. Appl. Cryst. **32**, 992–1002.

Wang, Y. M. and Ma, E. (**2004**). "Three strategies to achieve uniform tensile deformation in a nanostructured metal," Acta Mater. **52**, 1699–1709.

Wang, Y. M., Chen, M. W., Zhou, F. H., and Ma, E. (**2002**). "High tensile ductility in a nanostructured metal," Nature **419**, 912–915.

Wilkens, M. (**1970a**). "Fundamental aspects of dislocation theory," in *NBS spl pub, II:317*, edited by J. A. Simmons, R. de Wit, and R. Bullougs (US Department of Commerce, Washington, DC), p. 1195.

Wilkens, M. (**1970b**). "The determination of density and distribution of dislocations in deformed single crystals from broadened X-ray diffraction profiles," Phys. Status Solidi **2**, 359–363.

Williamson, G. K. and Hall, W. H. (**1952**). "X-ray line broadening from filed aluminium and wolfram," Acta Metal. **1**, 22–31.

Valiev, R. Z. (**1997**). "Structure and mechanical properties of ultrafine-grained metals," Mater. Sci. Eng. A **234–236**, 59–66.

Valiev, R. Z., Islamgaliev, R. K., and Alexandrov, I. V. (**2000**). "Bulk nanostructured materials from severe plastic deformation," Prog. Mater. Sci. **45**, 103–189.